

Electronic structure, charge density, and chemical bonding properties of $C_{11}H_8N_2O$ *o*-methoxydicyanovinylbenzene (DIVA) single crystal

A. H. Reshak · H. Kamarudin · I. V. Kityk · S. Auluck

Received: 12 February 2013 / Accepted: 7 March 2013 / Published online: 22 March 2013
© Springer Science+Business Media New York 2013

Abstract A comprehensive theoretical density functional theory (DFT) study of the electronic crystal structure, bonding properties, electron charge density of $C_{11}H_8N_2O$ *o*-methoxydicyanovinylbenzene (DIVA) single crystals were performed. The exchange and correlation potential was described within a framework of the local density approximation (LDA) by Ceperley–Alder and gradient approximation (GGA) based on exchange–correlation energy optimization to calculate the total energy. In addition, we have used Engel–Vosko generalized gradient approximation (EV-GGA) and the modified Becke–Johnson potential (mBJ) for the electronic crystal structure, bonding properties, electron charge density calculations. There is systematically increasing in the energy gap from 2.25 eV (LDA), 2.34 eV (GGA), 2.50 eV (EV-GGA), 2.96 eV (mBJ). Our calculations show that this crystal possess direct energy gap. Furthermore, the electronic charge density space distribution contours in the (1 1 0)

crystallographic plane clarifies the nature of chemical bonding.

Introduction

Structural data, along with theoretical calculations and experimental measurements, help to reveal the nature of the relevant structure property relationships. Structural studies of polarized organic molecules as components for hydrogen storage materials, nonlinear optical (NLO) and photorefractive materials have attracted a great deal of attention in the last two decades [1]. They have crucial advantages in comparison with currently used inorganic crystals [1]. The introduction of molecular asymmetry or chirality, is often the promising strategy to achieve centrosymmetric or non-centrosymmetric packing. The supramolecular packing will be governed by steric interactions and van der Waals forces. In crystals, molecules are linked by non-covalent intermolecular interactions like electrostatic interactions, hydrogen bonds, and van der Waals ones [2–9]. Molecules tend to undergo shape simplification during crystal growth, which gives rise to dimers and then to high-order aggregates to adapt to a close-packing in the solid state. The high tendency of achiral molecules to crystallize centrosymmetrically could be due to such a close-packing driving force. Therefore, if the symmetry of the chromophores is reduced, dimerization and subsequent aggregation is no longer of advantage to the close-packing and increases probability of acentric crystallization. This symmetry reduction can be accomplished either by introduction of molecular (structural) asymmetry or incorporation of steric (bulky) substituents into the chromophore. In addition, hydrogen bond functionalities may be included to promote a desired chromophore packing. Coulomb inter-molecular forces are used

A. H. Reshak (✉)
Institute of Complex Systems, FFPW, CENAKVA, University of South Bohemia in CB, 37333 Nove Hradky, Czech Republic
e-mail: maaidph@yahoo.co.uk

A. H. Reshak · H. Kamarudin
School of Material Engineering, Malaysia University of Perlis,
P.O. Box 77, d/a Pejabat Pos Besar, 01007 Kangar, Perlis,
Malaysia

I. V. Kityk
Electrical Engineering Department, Technological University of Czeszochowa, Al. Armii Krajowej 17/19, Czeszochowa, Poland

S. Auluck
Council of Scientific and Industrial Research - National Physical Laboratory, Dr. K S Krishnan Marg, New Delhi 110012, India

for charged chromophores in combination with counter-ions that tend to override the weaker dipole–dipole interactions and promote a non-centrosymmetric packing. This is especially the case for second-order NLO crystals where a non-centrosymmetric arrangement of molecules is required [10–12]. For NLO crystals, it is very well known that a different orientation of chromophores essentially affects the macroscopic NLO properties [13, 14].

The band energy theoretical methods for studying the relationship between structure and the optical properties may sometimes be a better solution before venturing into the physical growth of the crystals. The ab initio calculations have been extensively used for the computations of structural parameters. In recent years, density functional theory (DFT) has become an increasingly useful tool to interpret experimental studies. The success of DFT is mainly due to the fact that it describes small molecules more reliably than Hartree–Fock theory. It is also computationally more economical than wave function-based methods with inclusion of electron correlations [15, 16]. The present study is an attempt to understand an interesting biologic system. We present calculations that are based on the full potential linear augmented plane wave (FP-LAPW) method which has proven to be one of the accurate methods [17, 18] for the computation of the electronic structure of solids within a framework of DFT. Such a study is all the more interesting as the structure of this single crystal has been determined by Mikhael et al. [19] using X-ray diffraction. Beyond this, not much is known about this crystal. We hope that our study will be a step in this direction.

In the next section, we briefly describe the calculation procedure and give the computational details. In Sect. [Results and discussion](#), we report and discuss our result. Finally, conclusions will be given in Sect. [Conclusions](#).

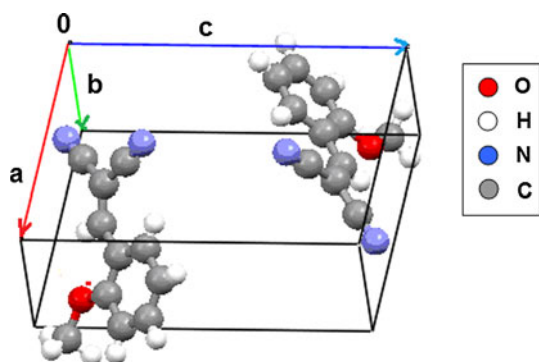
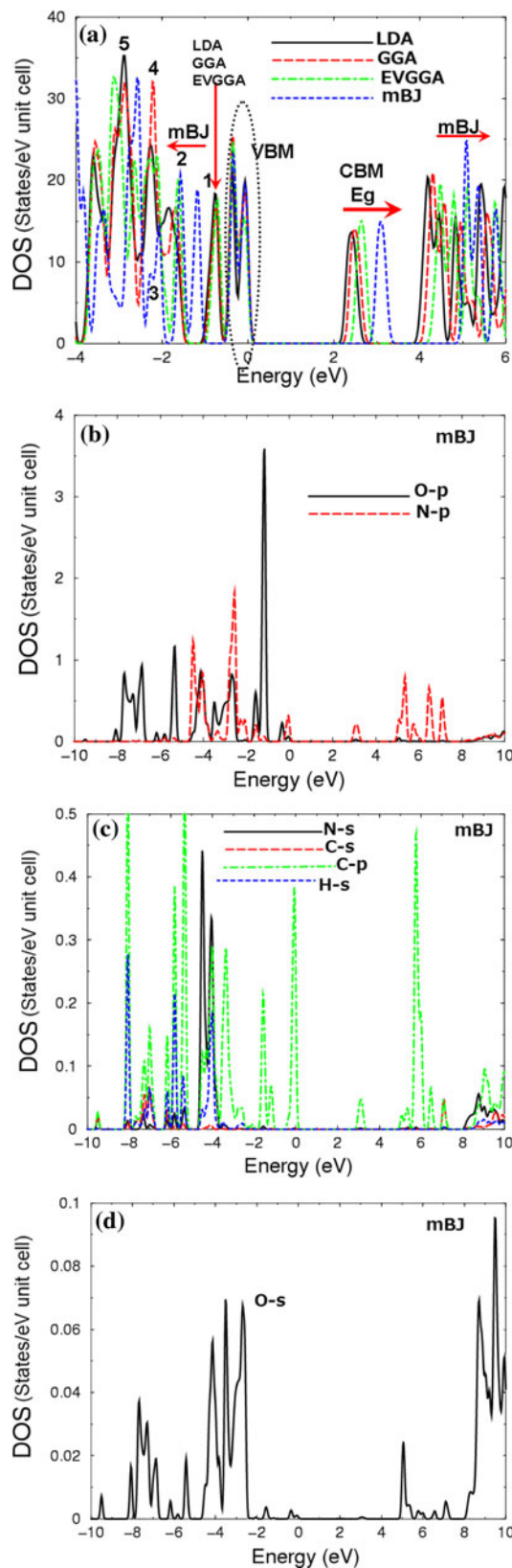


Fig. 1 The unit cell of DIVA



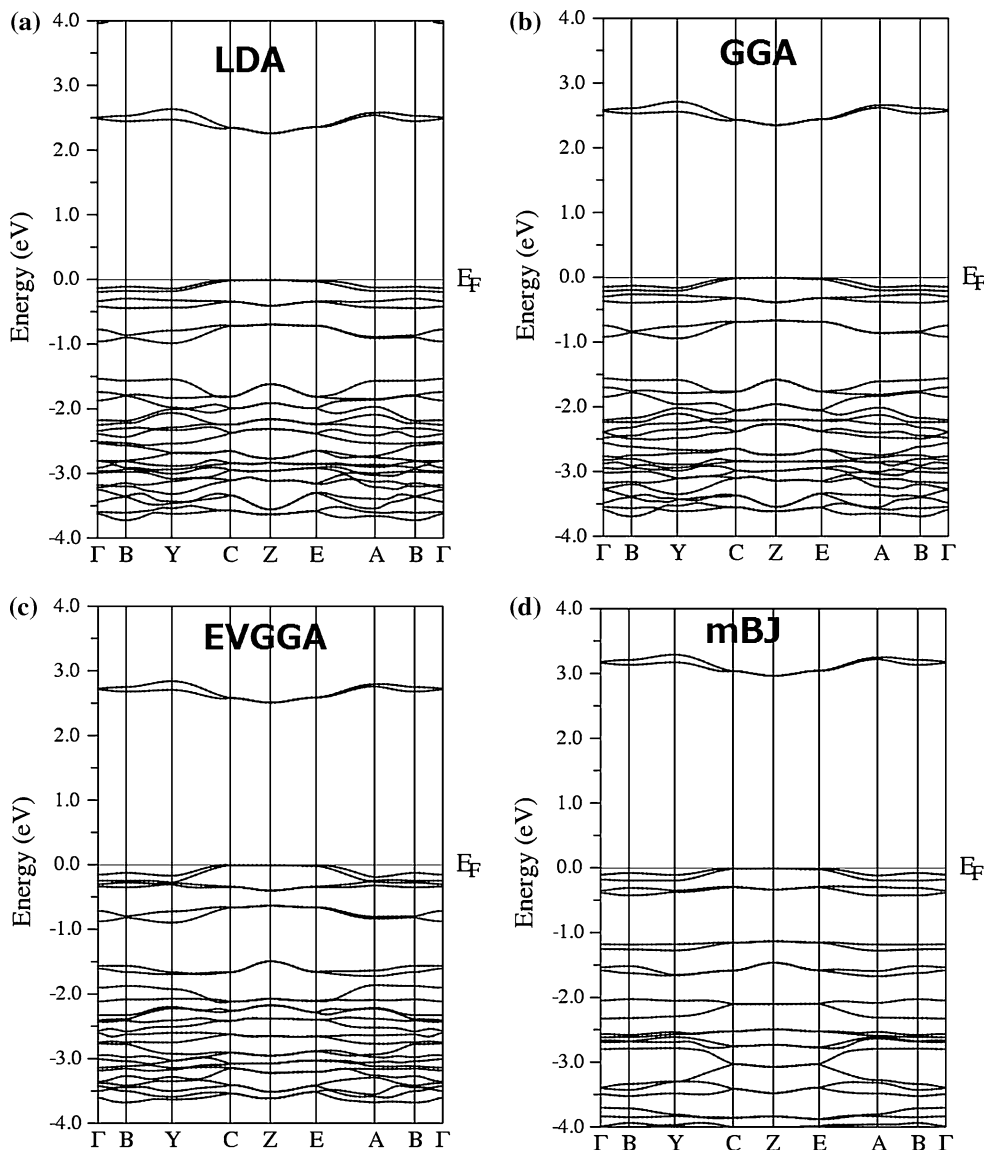
◀ **Fig. 2** Calculated total and partial densities of states (states/eV unit cell). **a** Total densities of states using LDA, GGA, EV-GGA, and mBJ, **b–d** partial densities of states using mBJ

Structural properties and computational details

$C_{11}H_8N_2O$ *O*-methoxydicyanovinylbenzene (DIVA) single crystals forms acentric monoclinic crystals (space group *P*21) with two formulas per unit cell. The unit cell dimensions are: $a = 7.922(2) \text{ \AA}$, $b = 5.402(2) \text{ \AA}$, $c = 11.375(2) \text{ \AA}$ and $\beta = 93.58(2)^\circ$. The crystal structure of $C_{11}H_8N_2O$ *o*-methoxydicyanovinylbenzene (DIVA) crystals is illustrated at Fig. 1. The X-ray crystallographic data taken from Ref. [19] were optimized by minimization of the forces (1 mRy/au) acting on the atoms. From the relaxed geometry the electronic structure and the chemical bonding can be

determined and various spectroscopic features can be simulated and compared with experimental data. The self-consistent density at these positions can be found after the forces are minimized by turning off the relaxations and driving the system to achieve self-consistency. Calculations are performed using the all-electron full potential linearized augmented plane wave (FP-LAPW) method [20]. This is an implementation of the DFT [21] with different possible approximation for the exchange correlation (xc) potentials. Exchange and correlation potential was described by the local density approximation (LDA) by Ceperley-Alder (CA) [22, 23] and gradient approximation (GGA) [24], which is based on exchange–correlation energy optimization to calculate the total energy. In addition, we have used Engel–Vosko generalized gradient approximation (EV-GGA) [25]

Fig. 3 The calculated band structure using. **a** LDA which give the energy gap values of about 2.25 eV, **b** GGA which give the energy gap values of about 2.34 eV, **c** EV-GGA which give the energy gap values of about 2.50 eV, **d** mBJ which give the energy gap values of about 2.96 eV



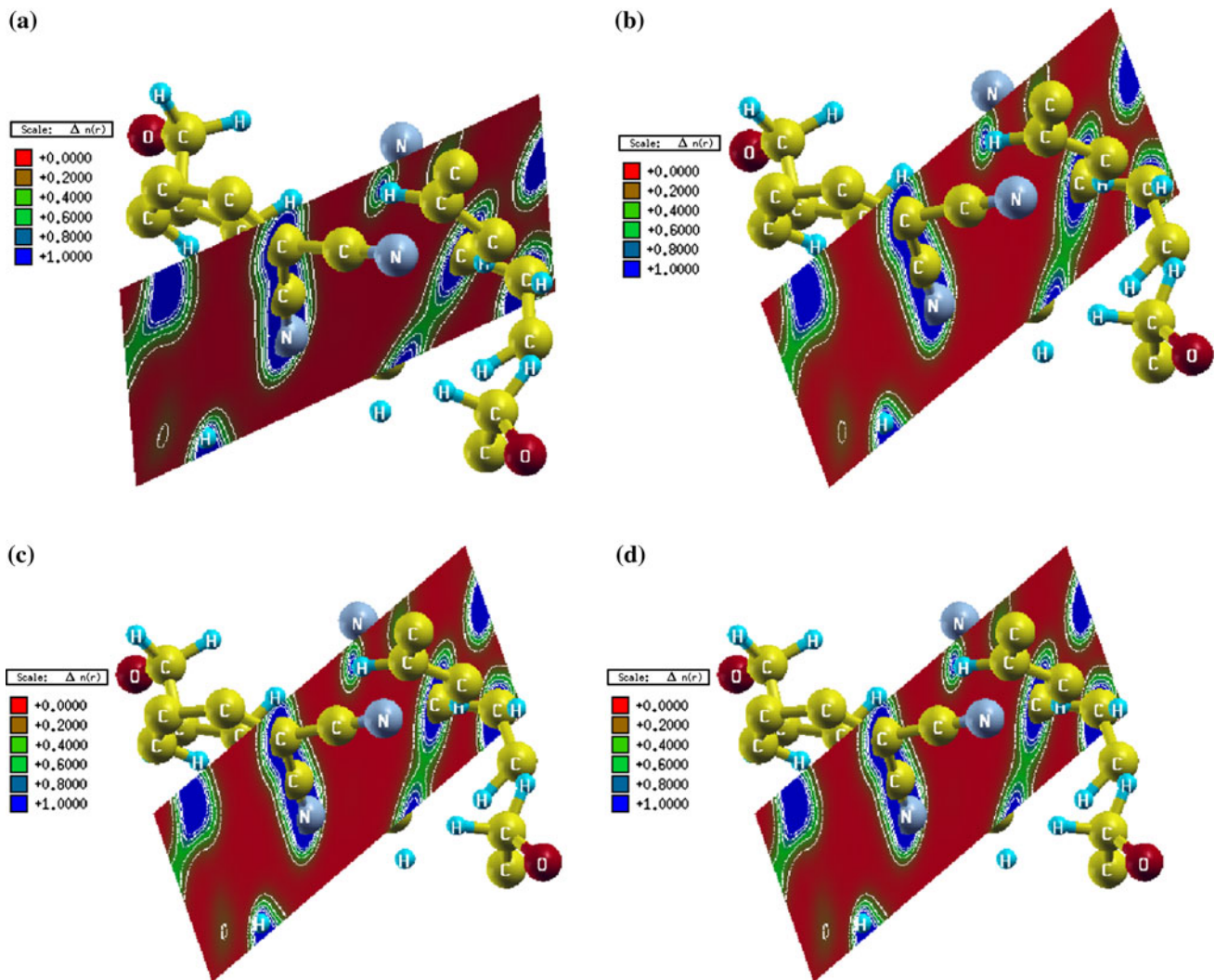


Fig. 4 Electronic space charge density distribution contour in the (1 1 0) plane. **a** LDA, **b** GGA, **c** EV-GGA, **d** mBJ. One can be observed from $\Delta n(r)$ the scale of the charge density colors where blue color has the maximum charge accumulation site

and the modified Becke–Johnson potential (mBJ) [26], which optimizes the corresponding potential for electronic band structure calculations. Our calculations will demonstrate the effect of the four different kinds of exchange–correlation potentials on the electronic band structure, density of states and the electronic space charge density distribution. The muffin-tin radius (R_{mt}) for C, H, N, O, and S were chosen in such a way that the spheres did not overlap at all. In order to get the total energy convergence, the basis functions in the interstitial regions (IR) were expanded up to $R_{mt} \times K_{max} = 7.0$ and inside the atomic spheres is the wave function. The maximum value of l were taken as $l_{max} = 10$, while the charge density is Fourier expanded up to $G_{max} = 20/a.u.$ We have used 35 k-points in the irreducible Brillouin zone (IBZ) for structural optimization. For the calculation of electronic properties 180 k-points within the BZ were used.

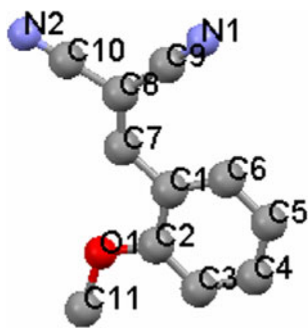
Results and discussion

Band structure and density of states

Four types of xc potentials were used to calculate the total density of states (TDOS) and the angular momentum decomposition of the atoms projected density of states (PDOS). These are presented in Fig. 2. In addition, the electronic band structure dispersion in \mathbf{k} -space along the high symmetry directions in the IBZ were evaluated and depicted in Fig. 3. The valence band maximum (VBM) and the conduction band minimum (CBM) are located at Z point of the BZ resulting in a direct band gap. It is well known that the DFT calculations underestimate the value of the energy gap. To overcome the well-known underestimation of LDA and GGA, we have used EV-GGA and mBJ which have been verified to obtain the calculated energy gap close to the

Table 1 Selected calculated bond lengths (Å) in comparison with experimental data [19]

Bond lengths	Exp.	Theory
C1–C2	1.415(3)	1.402
C1–C6	1.403(3)	1.399
C1–C7	1.451(2)	1.430
C2–C3	1.396(2)	1.389
C3–C4	1.379(3)	1.359
C4–C5	1.390(3)	1.381
C5–C6	1.386(2)	1.370
C7–C8	1.357(2)	1.350
C8–C9	1.435(3)	1.429
C8–C10	1.444(2)	1.438
C9–N1	1.143(3)	1.139
C10–N2	1.142(2)	1.138
O1–C2	1.353(2)	1.349
O1–C11	1.431(2)	1.428



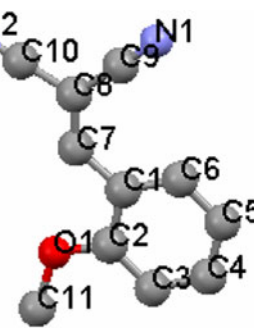
experimental one. Following Figs. 2 and 3, we notice that there is systematically increasing the energy gaps from 2.25 eV (LDA), 2.34 eV (GGA), 2.50 eV (EV-GGA), and 2.96 eV (mBJ). Fig. 2a, shows the influence of using different xc on the band gap, VBM, CBM and the other bands/structures as follow: (i) the VBM shows the same structure for the four xc. (ii) the CBM shows significant spectral shift toward the higher energies with respect to E_F when we move from LDA to GGA, EV-GGA, mBJ. (iii) the first structure under the VBM (labeled by # 1) remains at same position for LDA, GGA, and EV-GGA while it is shifted by around 0.5 eV for mBJ. (iv) for the structure labeled by #2, mBJ and EV-GGA give almost the same result, while there is significant shift for LDA structure toward lower energies. (v) for structure #3 mBJ is shifted toward higher energies with respect to LDA, GGA, and EV-GGA approaches. At structure #4, mBJ shows very small magnitude and also is shifted toward higher energies. Structure #5 shows mBJ shifts toward higher energies and EV-GGA toward lower energies. We have found that mBJ gives a better band gap value and corresponding bands splitting. Thus, we will show our results using mBJ only. If we look at the PDOS at Fig. 2b, c, d, we should notice that there is a strong hybridization between O-2p states and N-2p states around -4.0 , -3.0 , and -2.0 eV. Also there is a strong hybridization between H-1s states and C-2p states around -6.5 , -6.0 , -5.5 , and -4.0 eV. Finally, C-2s states hybridized with N-2s and C-2p states around -7.0 eV, and N-2s states with C-2p and H-1s states at around -4.0 eV.

Electronic space charge density distribution

The electronic charge density contours in the crystallographic plane (1 1 0) are illustrated in Fig. 4. Following

Table 2 Selected calculated bond angles ($^\circ$), in comparison with experimental data [19]

Bond angles	Exp.	Theory
C2–C1–C6	118.5(1)	118.0
C2–C1–C7	116.5(2)	116.1
C6–C1–C7	125.0(2)	124.6
C1–C2–C3	120.2(2)	119.7
C1–C2–O1	116.0(1)	115.7
C3–C2–O1	123.8(2)	123.5
C2–C3–C4	119.6(2)	118.8
C3–C4–C5	121.3(1)	120.8
C4–C5–C6	119.5(2)	119.0
C1–C5–C6	120.9(2)	120.4
C1–C7–C8	129.7(2)	129.1
C7–C8–C9	126.7(1)	126.1
C7–C8–C10	119.0(2)	118.7
C9–C8–C10	114.2(2)	113.9
C8–C9–N1	177.6(2)	177.2
C8–C10–N2	179.2(3)	178.9
C2–O1–C11	118.5(1)	118.0



these contours the origin of chemical bonds between all atoms can be clarified. Depending on Pauling electronegativity values, we can classify the type of the bonding between the atoms. The titled crystal contains C (electronegativity value = 2.55), H (2.20), N (3.04) and O (3.44). Accordingly, the bonds between C–C are covalent, whereas the bonds C–N, C–O, C–H, and O–H are ionic due to the large electro-negativity values between these atoms. Since O and N show the large Pauling electro-negativity values that mean the majority of charges are accumulated on O and N atomic site positions and the distribution of electronic charge is almost spherical. We also should emphasize that the valence electrons from H and C sites are transferred to O and N sites. This can be observed from $\Delta n(r)$ the scale of the charge density colors where blue color has the maximum charge accumulation site (see Fig. 4). The bond lengths and the bond angles were calculated and compared with the experimental data [19] (see Table 1, 2; Fig. 1b).

Conclusions

In summary, a DFT calculation for the electronic crystal structure, bonding properties, electron charge densities, for $C_{11}H_8N_2O$ *o*-methoxydicyanovinylbenzene (DIVA) single crystals were performed using the FP-LAPW method within WIEN2 K code. Four different xc potentials were used. There is systematically increasing the energy gap values from 2.25 eV (LDA), 2.34 eV (GGA), 2.50 eV

(EV-GGA), 2.96 eV (mBJ). The chemical bonding is investigated through the electronic charge density space distribution contours in the (1 1 0) crystallographic plane.

Acknowledgements This study was supported from the institutional research concept of the project CENAKVA (No. CZ.1.05/2.1.00/01.0024), the grant No. 152/2010/Z of the Grant Agency of the University of South Bohemia. The School of Materials Engineering, University Malaysia Perlis (UniMAP), Perlis, Malaysia. S.A. thanks Council of Scientific and Industrial Research (CSIR) - National Physical Laboratory for financial support.

References

1. Zyss J., Ledoux I., Nicoud J. F. (1994). *Mole*
2. Desiraju GR (2002) *Acc Chem Res* 35:565
3. Aakeroy CB, Seddon KR (1993) *Chem Soc Rev* 22:397
4. Saha BK, Nangia A, Jaskolski M (2005) *Cryst Eng Comm* 7:355
5. Russell VA, Etter MC, Ward MD (1994) *J Am Chem Soc* 116: 1941
6. Huang KS, Britton D, Etter MC, Byrn SR (1995) *J Mater Chem* 5:379
7. Panunto TW, Urbanczyk-Lipkowska Z, Johnson R, Etter MC (1987) *J Am Chem Soc* 109:7786
8. R. Custelcean, *Chem. Commun. (Cambridge)* 2008, 295
9. Yin Z, Li Z (2006) *Tetrahedron Lett* 47:7875
10. Jazbinsek M, Kwon OP, Bosshard Ch, Günter P (2008) handbook of organic electronics and photonics. In: Nalwa SH (ed), American Scientific Publishers, Los Angeles
11. Bosshard Ch, Bösch M, Liakatas I, Jäger M, Günter P (2000) Nonlinear optical effects and materials. In: Günter P (ed), Springer, Berlin
12. Nalwa HS, Watanabe T, Miyata S (1997) Nonlinear optics of organic molecules and polymers. In: Nalwa HS, Miyata S (eds), CRC, Boca Raton
13. Zyss J, Oudar JL (1982) *Phys Rev A* 26:2028
14. Kwon O-P, Jazbinsek M, Seo J-I, Choi E-Y, Yun H, Fabian DJ, Brunner Y, Lee S, Günter P (2009) *J Chem Phys* 130:134708
15. Koch W, Holthausen MCAA (2000) *Chemistry guide to density functional theory*. Wiley, Weinheim
16. Parr RR, Yang RG (1989) *Density functional theory of atoms and molecules*. Oxford University Press, New York and references therein
17. Gao S (2003) *Comput Phys Commun* 153:190
18. Schwarz K (2003) *J Solid State Chem* 176:319
19. Antipin MY, Barr AT, Cardelino HB, Clark DR, Moore EC, Myers T, Penn B, Romero M, Timofeeva VMST (1997) *J Phys Chem B* 101:2770
20. Blaha P, Schwarz K, Madsen GKH, Kvasnicka D, Luitz J (2001) WIEN2 K, an augmented plane wave + local orbitals program for calculating crystal properties, Karlheinz Schwarz. Techn Universität Wien, Wien. ISBN 3-9501031-1-2
21. Hohenberg P, Kohn W (1964) *Phys Rev B* 136:864
22. Ceperley DM, Ader BI (1980) *Phys Rev Lett* 45:566
23. Perdew JP, Zunger A (1973) *Phys Rev B* 8:4822
24. Perdew JP, Burke S, Ernzerhof M (1996) *Phys Rev Lett* 77:3865
25. Engel E, Vosko SH (1993) *Phys Rev B* 47:13164
26. Tran F, Blaha P (2009) *Phys Rev Lett* 102:226401